

# Theoretical Study of Hyperpolarizabilities in Crystalline *m*-Nitroaniline

Hideharu Nobutoki\* and Hiroshi Koezuka

Advanced Technology R&D Center, Mitsubishi Electric Corporation, 1-1 Tsukaguchi-Honmachi 8-Chome, Amagasaki, Hyogo 661, Japan

Received: July 15, 1996; In Final Form: January 29, 1997<sup>⊗</sup>

A variational–perturbation method in terms of molecular orbitals (MOs) has been developed to study the effect of a permanent crystal field on hyperpolarizability ( $\beta$ ) in van der Waals organic crystals. The method has the advantage of giving a numerical value of the dipole moment for each fragment molecule in a weakly interacting system with an accuracy comparable to the supermolecule method. Our method has been applied to a *m*-nitroaniline molecule in different model crystal environments to analyze the crystal field effect on the  $\beta$ -values. The results indicate that the crystal field induces the intramolecular charge transfer (CT) of the  $\pi$ -electrons from an NH<sub>2</sub> group to a NO<sub>2</sub> group in the highest occupied MO while the lowest unoccupied MO almost remains unchanged. From a net atomic charge analysis, the CT will be derived from the reversed polarization of the  $\sigma$ -electrons due to the polarized  $\pi$ -electrons and it will then contribute to the enhancement of the  $\beta_x$ -value additively ( $\beta_{\text{add}}$ ). The effect of the different crystal environments on the  $\beta_{\text{xxx}}$ -values has been also discussed with a focus on the degree of the ground state polarization.

## 1. Introduction

Organic nonlinear optical materials have been intensively studied from scientific and practical standpoints for the last decade.<sup>1</sup> To understand nonlinear optical phenomena and/or to design new organic nonlinear optical materials theoretically, molecular orbital (MO) calculations of hyperpolarizability ( $\beta$ ) have been frequently performed.<sup>2</sup> Almost all the calculations have been carried out on individual molecules in van der Waals organic crystals. The second harmonic generation susceptibility  $\chi^{(2)}$  has been taken to be the sum of the individual molecular contributions.<sup>3</sup> In other words, the crystal field has been assumed to be negligible.<sup>4</sup> In some cases, this assumption may be justified. Particularly in polar crystals, however, a local electrostatic field due to the crystal may be quite important.<sup>5</sup> In such cases, a calculation of  $\beta$  should take the permanent crystal field into account.<sup>4,6–9</sup>

A typical example is crystalline *m*-nitroaniline (*m*-NA). The *m*-NA system is one of simple donor–acceptor molecules with a non-centrosymmetric van der Waals crystal structure, and its large optical nonlinearities in the crystalline state have been recognized.<sup>8,10,11</sup> In the crystal, hydrogen bonding (H–bonding) plays a significant role.<sup>12,13</sup> Thus, it is relevant to demonstrate theoretically the effect of the crystal field, derived from forces such as the H–bonding, on  $\beta$ . Our aim in this study is to explore theoretically the crystal field effect on  $\beta$  in van der Waals organic crystals.

One can see that there are two theoretical approaches to solving this problem on the basis of MO theory. One is a perturbation approach. However, only few calculations based on this method are reported. The usual perturbation method cannot describe the simultaneous interactions of more than two molecules, and therefore, it does not provide accurate results. The other is a supermolecule (SM) method.<sup>14</sup> This method, which is known to be more accurate, treats interacting molecules as one common supermolecule. Dirk *et al.* have indeed revealed the influence of H–bonding on the  $\beta$ -values of a urea dimer by using this method.<sup>4</sup> However, the treatment with the SM method is difficult for larger systems. It is not easy to analyze

well the influence on the  $\beta$  of each fragment molecule since the SM method only gives  $\beta$ -values of the “supermolecule”. As one successful approach to remedy this shortcoming of this method, Zyss and Berthier have demonstrated the influence of a urea crystal field on  $\beta$  by introducing Coulomb point-charge interaction potentials.<sup>6</sup>

In this paper, we also present alternative expressions based on a variational–perturbation method for determining the crystal field effect on the  $\beta$  for van der Waals organic crystals. To confirm the reliability of our method, dipole moments ( $\mu$ ) calculated by the method are compared with those by the conventional perturbation method and by the SM method. Our method has been applied to a crystalline *m*-NA molecule, that is, the molecule in a crystal. We present the  $\beta$ -values of the molecule in the different crystal environments of several model crystals. The crystal field effect on the  $\beta$ -values has been analyzed and discussed in terms of frontier molecular orbitals, namely, highest occupied MO (HOMO) and lowest unoccupied MO (LUMO),  $\mu$ , and net atomic charges.

## 2. Method of Computation

Our aim in this section is to construct an effective Hamiltonian which renormalizes a weak intermolecular interaction derived from the van der Waals force. Let us consider a composite system consisting of three weakly interacting molecules A, B, and C, namely, a three-body problem, as one example of explaining our method for the sake of simplicity. Here one separates the interacting molecular space into three subspaces, A, B, and C. The molecular eigenvalue equation for the system can then be written in block matrix notation as follows

$$\begin{bmatrix} \mathbf{F}_{AA} & \mathbf{F}_{AB} & \mathbf{F}_{AC} \\ \mathbf{F}_{BA} & \mathbf{F}_{BB} & \mathbf{F}_{BC} \\ \mathbf{F}_{CA} & \mathbf{F}_{CB} & \mathbf{F}_{CC} \end{bmatrix} \begin{bmatrix} \mathbf{C}_A \\ \mathbf{C}_B \\ \mathbf{C}_C \end{bmatrix} = \epsilon \begin{bmatrix} \mathbf{S}_{AA} & \mathbf{S}_{AB} & \mathbf{S}_{AC} \\ \mathbf{S}_{BA} & \mathbf{S}_{BB} & \mathbf{S}_{BC} \\ \mathbf{S}_{CA} & \mathbf{S}_{CB} & \mathbf{S}_{CC} \end{bmatrix} \begin{bmatrix} \mathbf{C}_A \\ \mathbf{C}_B \\ \mathbf{C}_C \end{bmatrix} \quad (1)$$

where  $\mathbf{F}_{PQ}$  and  $\mathbf{S}_{PQ}$ , ( $P, Q = A, B, \text{ and } C$ ), represent Fock and overlap matrices between the molecules  $P$  and  $Q$ , respectively.  $\mathbf{C}_P$ , ( $P = A, B, \text{ and } C$ ), stands for the coefficient matrix. The intermolecular interaction is so small in van der Waals organic crystals that the overlap matrix between the different molecules

<sup>⊗</sup> Abstract published in *Advance ACS Abstracts*, April 15, 1997.

can be approximated as

$$\mathbf{S}_{PQ} = \delta_{PQ} \quad (2)$$

where  $\delta_{PQ}$  denotes the Kronecker  $\delta$ . We further assume that only direct intermolecular interaction need be taken into account, that is, indirect interactions may be neglected. When our attention is focused on molecule A, this approximation can be described by

$$\mathbf{F}_{BC} = \mathbf{F}_{CB} = \mathbf{0} \quad (3)$$

The matrix eigenvalue equation for the A-molecule is then reduced into

$$\begin{bmatrix} \mathbf{F}_{AA} & \mathbf{F}_{AB} & \mathbf{F}_{AC} \\ \mathbf{F}_{BA} & \mathbf{F}_{BB} & \mathbf{0} \\ \mathbf{F}_{CA} & \mathbf{0} & \mathbf{F}_{CC} \end{bmatrix} \begin{bmatrix} \mathbf{C}_A \\ \mathbf{C}_B \\ \mathbf{C}_C \end{bmatrix} = \epsilon \begin{bmatrix} \mathbf{C}_A \\ \mathbf{C}_B \\ \mathbf{C}_C \end{bmatrix} \quad (4)$$

The  $\mathbf{C}_B$  and  $\mathbf{C}_C$  variables are easily transformed to give an effective matrix eigenvalue equation for the A-molecule as follows

$$[\mathbf{F}_{AA} + \mathbf{F}_{AB}(\epsilon \cdot \mathbf{I}_B - \mathbf{F}_{BB})^{-1}\mathbf{F}_{BA} + \mathbf{F}_{AC}(\epsilon \cdot \mathbf{I}_C - \mathbf{F}_{CC})^{-1}\mathbf{F}_{CA}] \mathbf{C}_A = \epsilon \mathbf{C}_A \quad (5)$$

where  $\mathbf{I}_B$  and  $\mathbf{I}_C$  represent the unit matrix. This transformation is known as Löwdin partitioning of the Hamiltonian.<sup>15</sup> Equation 5 can be regarded as the extension of the Brillouin–Wigner perturbation method.<sup>16</sup> This equation can be written in a simple form as

$$\mathbf{H}_{AA}(\epsilon) \mathbf{C}_A = \mathbf{0} \quad (6)$$

where

$$\mathbf{H}_{AA}(\epsilon) = \mathbf{F}_{AA} + \mathbf{F}_{AB}(\epsilon \cdot \mathbf{I}_B - \mathbf{F}_{BB})^{-1}\mathbf{F}_{BA} + \mathbf{F}_{AC}(\epsilon \cdot \mathbf{I}_C - \mathbf{F}_{CC})^{-1}\mathbf{F}_{CA} - \epsilon \quad (7)$$

The Hamiltonian matrix  $\mathbf{H}_{AA}$  is explicitly a function of the eigenvalue  $\epsilon$  for the A-molecule. The second and the third terms on the right hand side of eq 7 are constructed with the MOs ( $\phi_B$  and  $\phi_C$ ) and the orbital energies ( $\epsilon_B$  and  $\epsilon_C$ ) of the interacting partner molecules. Therefore, the matrix  $\mathbf{H}_{AA}$  depends on the parameters of those MOs and their orbital energies,

$$\mathbf{H}_{AA}(\epsilon; \phi_B, \epsilon_B; \phi_C, \epsilon_C) \mathbf{C}_A = \mathbf{0} \quad (8)$$

The inverse matrices  $(\epsilon \cdot \mathbf{I}_B - \mathbf{F}_{BB})^{-1}$  and  $(\epsilon \cdot \mathbf{I}_C - \mathbf{F}_{CC})^{-1}$  present major computational difficulties in solving eq 8. They have been considered in detail by several authors. The ways considered to overcome this difficulty include a variety of familiar quantum mechanical approximation methods. In this study, the Brillouin–Wigner perturbation expansion has been employed to overcome the difficulty.<sup>17</sup> Alternatively, if  $\mathbf{F}_{AB}$  and  $\mathbf{F}_{AC}$  are regarded as perturbing potentials, the inverse matrices can be identified as a Green function.<sup>18</sup> For example, the inverse matrix  $(\epsilon \cdot \mathbf{I}_B - \mathbf{F}_{BB})^{-1}$  can be rewritten as a power series expansion

$$\begin{aligned} (\epsilon \cdot \mathbf{I}_B - \mathbf{F}_{BB})^{-1} &= [(\epsilon \cdot \mathbf{I}_B - \mathbf{F}_{BB}^d) - \mathbf{F}_{BB}^{\text{off}}]^{-1} \\ &= (\epsilon \cdot \mathbf{I}_B - \mathbf{F}_{BB}^d)^{-1} + (\epsilon \cdot \mathbf{I}_B - \mathbf{F}_{BB}^d)^{-1} \\ &\quad \mathbf{F}_{BB}^{\text{off}}(\epsilon \cdot \mathbf{I}_B - \mathbf{F}_{BB}^d)^{-1} + \dots \quad (9) \end{aligned}$$

where  $\mathbf{F}_{BB}^d$  and  $\mathbf{F}_{BB}^{\text{off}}$  denote the diagonal (nonperturbative)

and the off-diagonal (perturbative) matrices, respectively. Equation 8 for the A-molecule can then be variationally solved by using eq 9 as a conventional secular equation. The similar equations for B- and C-molecules can be derived according to the above procedure to give

$$\mathbf{H}_{PP}(\epsilon; \phi_Q, \epsilon_Q; \phi_R, \epsilon_R) \mathbf{C}_P = \mathbf{0}; \quad P \neq Q \neq R \neq A, B, \text{ and } C \quad (10)$$

Equation 10 is iteratively (Brillouin–Wigner perturbation method like) solved for the three molecules until the orbital energies of each of the molecules in the system have converged

$$\begin{aligned} \mathbf{H}_{PP}^{(N)}(\epsilon^{(N)}; \phi_Q^{(N-1)}, \epsilon_Q^{(N-1)}; \phi_R^{(N-1)}, \epsilon_R^{(N-1)}) \mathbf{C}_P = \mathbf{0}, \\ |\epsilon_P^{(N)} - \epsilon_P^{(N-1)}| < \Delta_P^{(N)}; \\ P \neq Q \neq R \neq A, B, \text{ and } C \quad (11) \end{aligned}$$

where  $N (\geq 1)$  and  $\Delta_P^{(N)}$  indicate the number of the iteration and the convergence criterion vector, respectively. Iteration here means repeated application of the Brillouin–Wigner perturbation theory. The weak intermolecular interactions are renormalized into the new MOs and their eigenenergies by the iteration.<sup>19</sup> The  $\phi_P^{(N)}$  is related to the  $\phi_P^{(N-1)}$  through the expansion coefficient matrix  $\mathbf{U}_P^{(N-1)}$  as follows:

$$\phi_P^{(N)} = \mathbf{U}_P^{(N-1)} \phi_P^{(N-1)} \quad \text{for } \epsilon_P^{(N)}; \quad P = A, B, \text{ and } C \quad (12)$$

The  $\phi_P^{(N)}$  can be rewritten in terms of the  $\phi_P^{(0)}$  by

$$\begin{aligned} \phi_P^{(N)} &= \mathbf{U}_P^{(N-1)} \mathbf{U}_P^{(N-2)} \dots \mathbf{U}_P^{(2)} \mathbf{U}_P^{(1)} \phi_P^{(0)} \\ &= \mathbf{U}'_P^{(N-1)} \phi_P^{(0)} \quad \text{for } \epsilon_P^{(N)}; \\ &\quad P = A, B, \text{ and } C \quad (13a) \end{aligned}$$

where

$$\mathbf{U}'_P^{(N-1)} = \mathbf{U}_P^{(N-1)} \mathbf{U}_P^{(N-2)} \dots \mathbf{U}_P^{(2)} \mathbf{U}_P^{(1)} \quad (13b)$$

Equation 13 shows that the  $\phi_P^{(N)}$  is represented by a linear combination of the isolated (non-intermolecular interacting) MOs  $\phi_P^{(0)}$ . The wave function  $\Phi$  of the whole system can be described as the following simple product

$$\Phi = |\phi_A^{(N)}\rangle \cdot |\phi_B^{(N)}\rangle \cdot |\phi_C^{(N)}\rangle \quad (14)$$

where  $|\phi_P^{(N)}\rangle$ , ( $P = A, B, \text{ and } C$ ), denotes the Slater determinant of the MOs  $\phi_P^{(N)}$ . It should be noted that the wave function  $\Phi$  involves electrostatic and polarization interactions since the overlap matrix between the different molecules is omitted as shown in eq 2. The above equations describe the three weakly interacting molecular systems. For a system consisting of more than three weakly interacting molecules, the corresponding equations are easily extended.

In this approach, weakly interacting molecules can be treated as free (independent) molecules in appearance since the intermolecular interaction is simply renormalized into each fragment molecule. We refer to this method as the variational Brillouin–Wigner perturbation (VBWP) method. The calculations in practice were carried out by taking account of terms up to the second order in a power series expansion of the inverse matrix in eq 9. All the components of the convergence criterion vector  $\Delta_P^{(N)}$  were set to be  $10^{-6}$  eV in solving eq 11.

The dipole moment  $p_i$  of a molecule in the presence of a homogenous electric field  $E_i$  can be written as a power series

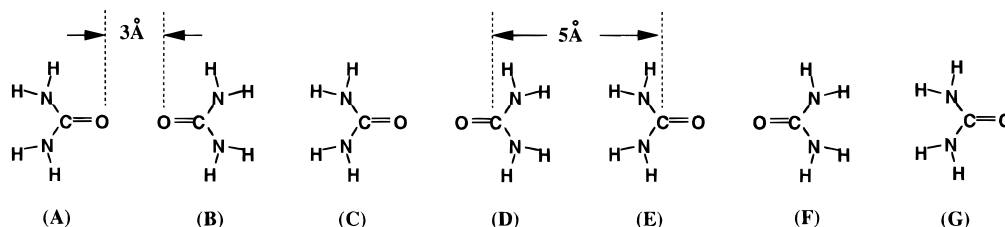


**Figure 1.** Assumed configuration of linearly aligned urea molecules.

**TABLE 1:  $\mu$ -Values (D) of Linearly Aligned Urea Molecules As Calculated by the VBWP, the Perturbation, and the Supermolecule Methods<sup>a</sup>**

number of molecules in the systems	VBWP method (perturbation method) <sup>b</sup>							total	supermolecule method
	A <sup>a</sup>	B <sup>a</sup>	C <sup>a</sup>	D <sup>a</sup>	E <sup>a</sup>	F <sup>a</sup>	G <sup>a</sup>		
2	-4.764 (-4.755)	4.764 (4.755)						0.000 (0.000)	0.000
3	-4.783 (-4.769)	4.631 (4.613)	-4.815 (-4.795)					-4.967 (-4.951)	-4.966
4	-4.776 (-4.764)	4.657 (4.631)	-4.657 (-4.631)	4.776 (4.764)				0.000 (0.000)	0.000
5	-4.778 (-4.766)	4.651 (4.627)	-4.676 (-4.645)	4.643 (4.622)	-4.812 (-4.793)			-4.972 (-4.955)	-4.971
6	-4.777 (-4.765)	4.654 (4.629)	-4.700 (-4.640)	4.700 (4.640)	-4.654 (-4.629)	4.777 (4.765)		0.000 (0.000)	0.000
7	-4.778 (-4.765)	4.653 (4.629)	-4.672 (-4.642)	4.664 (4.636)	-4.807 (-4.642)	4.644 (4.623)	-4.811 (-4.792)	-4.974 (-4.956)	-4.973

<sup>a</sup> The model structures are shown in Figure 1. <sup>b</sup> Values in parentheses indicate the  $\mu$ -values obtained by the second-order perturbation method of ref 25.

expansion in terms of the electric field

$$p_i = \mu_i + \alpha_{ij}E_j + (1/2)\beta_{ijk}E_jE_k + (1/6)\gamma_{ijkl}E_jE_kE_l + \dots \quad (15)$$

where  $\mu_i$  is a permanent dipole moment and tensors  $\alpha_{ij}$ ,  $\beta_{ijk}$ , and  $\gamma_{ijkl}$  stand for polarizability, hyperpolarizability, and second-order hyperpolarizability, respectively. The  $\beta_{ijk}$  have been calculated by numerical differentiation of the dipole moment  $p_i$ , which was obtained by using VBWP method, with respect to the electric field components in the limit of zero field, namely, the finite-field (FF) perturbation method. We have employed the FF method developed by Kurtz *et al.* to estimate the  $\beta_{ijk}$  and its vector part  $\beta_i$ .<sup>20</sup> It should be noted that static  $\beta$  are obtained from the FF calculations, while experimentally determined quantities are frequency-dependent. However, our approach remains meaningful especially since we are mainly interested in analyzing the effect of the crystal field on  $\beta$ .

All the calculations have been carried out on the basis of the self-consistent field—molecular orbital method at the level of CNDO/2 (complete neglect of differential overlap, version 2) approximation including all the valence electrons.<sup>21</sup> Ab initio MO calculations would be very costly and time consuming. The CNDO approximation is further convenient for the present study since it not only gives ground state charge distributions relatively well<sup>22</sup> but also, can easily fulfill the *invariance in space* requirement.<sup>23</sup>

### 3. Results and Discussion

**3.1. Reliability of The Method— $\mu$ -Values in Weakly Interacting Urea Molecules.** First, a calculation of  $\mu$ -values was performed on weakly interacting urea molecular systems by the VBWP method in order to confirm reliability of this method. A urea molecule is suitable for this study since it is known to be a simple and typical van der Waals organic crystal.

Figure 1 shows the assumed configuration of linearly aligned urea molecules studied. Two adjacent molecules in these systems are directed face to face in order to facilitate finding the degree of polarization derived from intermolecular interac-

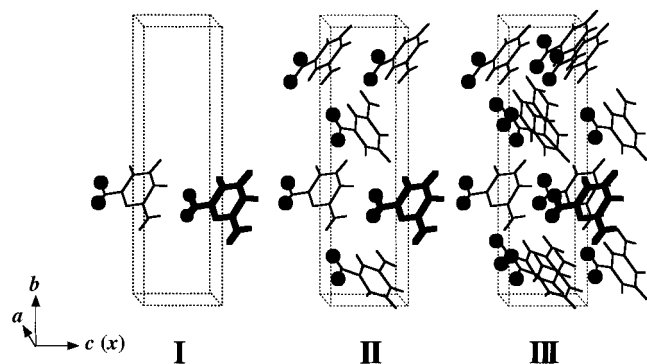
tions. The number of molecules included in the system was changed from two to seven. Intermolecular distances were assumed large enough to avoid intermolecular charge transfer (CT). Geometry of each urea molecule was taken from ref 24.

Table 1 indicates calculated  $\mu$ -values, where alphabetical characters in the upper row specify each molecule as shown in Figure 1. The calculated  $\mu$ -values by the perturbation and the SM methods are also shown in parentheses and in the right column, respectively. Here the perturbation method is that of Murrel *et al.*<sup>25</sup> This method includes terms up to the second order. It is denoted the MSP (Murrel's second-order perturbation) method. The MSP method includes terms to the same order as does the VBWP method.

As seen from the table, all the total  $\mu$ -values calculated by the VBWP method are in good agreement with those calculated by the SM method, while those by the MSP method disagree with those by the SM method. For each molecule in the system, the  $\mu$ -value obtained by the MSP method is fairly different from that obtained by the VBWP method. It has been clarified, from the above result, that the VBWP method correctly renormalizes the effect of the intermolecular interaction into the  $\mu$ -value of each molecule. It should be emphasized, in contrast to the SM method, that the VBWP method can clearly estimate the degree of a contribution of the  $\mu$ -value from each molecule to the total  $\mu$ -value in the whole system. In the case of the three interacting molecular system for example, the molecules A, B, and C are found to contribute -4.783, 4.631, and -4.815 D, respectively, to the total  $\mu$ -value of -4.967 D.

It has been confirmed that the VBWP method is superior to calculating a  $\mu$ -value (electron distribution) of each fragment molecule and that the method gives a total  $\mu$ -value with an accuracy comparable to the SM method. Thus, we have obtained a method for calculating reliable  $\beta$ -values of a crystalline *m*-NA molecule since  $\beta$ -values are estimated by numerical differentiation of  $\mu$ -values.

**3.2. A Crystalline *m*-NA Molecule.** **3.2.1.  $\beta$ -Values.** *m*-NA crystallizes in the space group *Pbc*2<sub>1</sub> and contains four molecules per unit cell.<sup>13</sup> Furthermore, in the crystal, H-bonding



**Figure 2.** Assumed model *m*-NA crystals. A molecule represented by bold lines stands for a reference molecule. The coordinate system was taken such that the *x*-axis coincides with the *c*-axis of a *m*-NA crystal, a perpendicular axis to the *x*-axis in the molecular plane of the reference molecule represents the *y*-axis, and that perpendicular to the *xy*-plane represents the *z*-axis. See text for the characteristics of the environment of the reference molecule in each of these model crystals.

**TABLE 2: Calculated  $\beta$ -Values (au) of an Isolated Molecule and of a Reference Molecule in the Model *m*-NA Crystals Studied by the VBWP Method Combined with the FF Method<sup>a</sup>**

model <sup>b</sup>	<i>xxx</i>	<i>xyy</i>	<i>xzz</i>	<i>yyy</i>	<i>yxx</i>	<i>yzx</i>	<i>x</i>	<i>y</i>	<i>z</i>
isolated	-457	122	-89	-45	-184	-122	-424	-351	-50
I	-853	101	-92	-75	-205	-116	-844	-396	-36
II	-300	189	-138	-88	-318	-15	-249	-421	-28
III	-593	96	-56	-63	-160	-280	-553	-503	-34

<sup>a</sup>  $\beta$ -Values on application on a perturbing field of  $10^{-3}$  au. <sup>b</sup> The model structures are shown in Figure 2.

effects appear to be important. These effects elude calculations within the  $\pi$ -electron approximation. The VBWP method has been applied to a *m*-NA molecule in different model crystal environments.

Figure 2 shows model *m*-NA crystals studied. Geometry and conformation of each *m*-NA molecule in the crystals were adapted from the experimental data of ref 13. A molecule represented by bold lines stands for a reference molecule. The coordinate system is taken such that the *x*-axis coincides with the *c*-axis of a *m*-NA crystal, a perpendicular axis to the *x*-axis in the molecular plane of the reference molecule represents the *y*-axis, and that perpendicular to the *xy*-plane represents the *z*-axis.

In each of these model crystals the environment of the reference molecule is different.<sup>12,13</sup> In I, NO<sub>2</sub> group oxygens of the reference molecule form bifurcated H-bondings with an NH<sub>2</sub> group of the neighboring molecule; the shortest intermolecular distance between the NO<sub>2</sub> group oxygen and the NH<sub>2</sub> group nitrogen (O–N(H)) is 3.250 Å. It should be remarked that the NH<sub>2</sub> group of the reference molecule in II makes a close contact with the NH<sub>2</sub> group of the adjacent molecule located below as shown in this figure. The distance N(H)–N(H) is 3.313 Å, and the shortest intermolecular distance among the hydrogens of the NH<sub>2</sub> groups is 2.044 Å. In III, which comprise the crystal II, all molecules associated with the unit cell are included in order to investigate the effect of an electrostatic field far from the reference molecule. Thus each reference molecule here specified is subject to different local crystal environments.

Table 2 lists calculated  $\beta$ -values of an isolated molecule and of a reference molecule in the model *m*-NA crystals studied by the VBWP method combined with the FF method. Note that, in obtaining the  $\beta$ -values, a maximum of 133 iterations of eq 11 were carried out in order to achieve convergence. As is apparent from this table, the  $\beta$ -value of each molecule changes

**TABLE 3: Mixing Coefficients of HOMO  $\phi_{\text{HOMO}}^{(N)}$  and of LUMO  $\phi_{\text{LUMO}}^{(N)}$  in the Expansion of the MOs in Terms of  $\phi_j^{(0)}$ s, the MOs of an Isolated Molecule**

isolated MOs <sup>b</sup> $\phi_j^{(0)}$	I <sup>a</sup>		II <sup>a</sup>		III <sup>a</sup>	
	$\phi_{\text{HOMO}}^{(N)}$	$\phi_{\text{LUMO}}^{(N)}$	$\phi_{\text{HOMO}}^{(N)}$	$\phi_{\text{LUMO}}^{(N)}$	$\phi_{\text{HOMO}}^{(N)}$	$\phi_{\text{LUMO}}^{(N)}$
LUMO + 2	— <sup>c</sup>	0.003	—	-0.008	0.007	0.017
LUMO + 1	—	—	—	-0.019	—	0.004
LUMO	-0.004	0.999	0.007	0.999	-0.001	0.999
HOMO	0.999	0.0004	0.996	-0.008	0.995	0.001
HOMO - 1	-0.031	-0.014	0.054	—	0.088	—
HOMO - 7	—	—	-0.051	-0.013	0.031	—

<sup>a</sup> The model structures are shown in Figure 2. <sup>b</sup> The MOs are schematically illustrated in Figure 3. <sup>c</sup> Bar indicates an absolute value smaller than 0.001.

considerably due to differences in the local crystal environments. Concerning a  $\beta_{\text{xxx}}$ -value, which lies along the direction of the crystal polar *c*-axis, the absolute value of the  $\beta_{\text{xxx}}$  in I is the largest value for the crystals studied. It is attributed to the H-bonding along the polar *x*-axis since the molecule in I is characterized by H-bonding as described above.

In comparison with the  $\beta_{\text{xxx}}$ -value in the isolated molecule, that in III increases by 1.30. The corresponding ratio is also 1.30 with respect to the  $\beta_x$ -value, which here denotes the averaged  $\beta$ -value along a crystal axis *c*. The ratio of 1.30 may seem not to be so large. However, the  $\beta$ -values obtained under the permanent crystal fields will be underestimated due to a lack of sufficiently diffuse basis functions and to an insufficient approximation of the CNDO in the present calculations.<sup>26</sup> Taking these factors into account, it may be considered that the crystal field has non-negligible influence on the  $\beta_x$ -value.

**3.2.2. Frontier Molecular Orbital Characteristics.** It has been known that frontier molecular orbitals play a dominant role in determining  $\beta$ .<sup>27–29</sup> This is particularly the case when the applied electric field is a small perturbation, as in the FF method.<sup>30</sup> Thus, we investigated the way in which the crystal field influences  $\beta$  through the shapes of the frontier orbitals.

Permanent crystal fields induce the orbital mixing between occupied and virtual orbitals of a molecule in its ground state. Hence the effect of the crystal fields on  $\beta$ -values may be estimated by the degree of the orbital mixing.<sup>31</sup> In the VBWP method, the degree of orbital mixing can easily be obtained from the expansion coefficient matrix  $U'_p^{(N-1)}$  in eq 13b. Table 3 summarizes mixing coefficients of HOMO  $\phi_{\text{HOMO}}^{(N)}$  and of LUMO  $\phi_{\text{LUMO}}^{(N)}$  in the expansion of these MOs in terms of  $\phi_j^{(0)}$ s, the MOs of an isolated molecule. Here the  $\phi_j^{(0)}$ s, which mainly contribute to the  $\phi_{\text{HOMO}}^{(N)}$ , are schematically illustrated in Figure 3. This table reveals that the crystal fields only affect the  $\phi_{\text{HOMO}}^{(N)}$  since the  $\phi_{\text{LUMO}}^{(N)}$  is almost composed of the  $\phi_{\text{LUMO}}^{(0)}$ .

To examine the orbital mixing characteristics in the  $\phi_{\text{HOMO}}^{(N)}$ , its linear combination of atomic orbitals (LCAO) coefficients were estimated. Figure 4 shows the LCAO coefficients of  $\phi_{\text{HOMO}}^{(N)}$  in II and in III. Although the variations in the LCAO coefficients are very small, even these differences may influence polarization properties.<sup>28,31a</sup> This would be supported by the fact that the differences lead to the non-negligible variations in the orbital energies of  $\phi_{\text{HOMO}}^{(N)}$ , as presented in Table 4. As seen from the comparisons of the LCAO coefficients, the HOMO in III gives relatively higher electron density on the NO<sub>2</sub> group and relatively lower electron density on the NH<sub>2</sub> group than is the case in II. In other words, the crystal field of III induces the intramolecular CT of the  $\pi$ -electrons from the NH<sub>2</sub> group to the NO<sub>2</sub> group in the HOMO. This CT implies

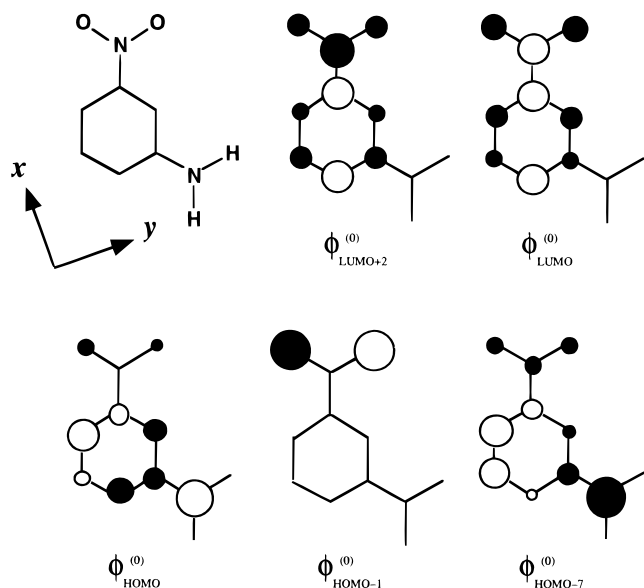


**Figure 3.** Schematic illustration of the MOs  $\phi^{(i)}$ , which mainly contribute to the  $\phi^{(N)}$ , of an isolated molecule in the absence of a static electric field.  $\phi^{(i)}$  represents a MO with  $i$ th lower orbital level than the HOMO level and  $\phi^{(j)}$  a MO with  $j$ th higher orbital level than LUMO level.

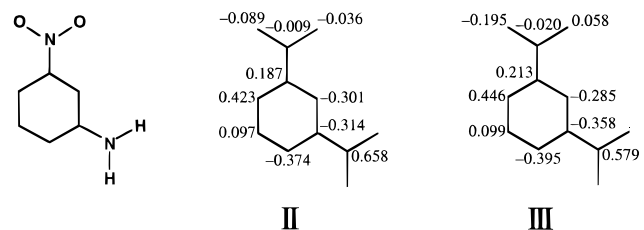


**Figure 4.** LCAO coefficients of the  $\phi^{(N)}$  of a reference molecule in the model  $m$ -NA crystals II and III.

**TABLE 4: The HOMO and the LUMO Level Energies (eV) of an Isolated Molecule and of a Reference Molecule in the Model  $m$ -NA Crystals Studied**

model <sup>a</sup>	$\epsilon(\text{HOMO})$	$\epsilon(\text{LUMO})$
isolated	-12.24	1.26
I	-12.73	0.79
II	-11.18	1.86
III	-12.34	1.37

<sup>a</sup> The model structures are shown in Figure 2.

that the induced polarization by the mixing of the HOMO and the LUMO may be less reduced in the reference molecule of III than that in the reference molecule of II since the CT decreases the donor character of the  $\pi$ -electrons on the HOMO before application of optical fields.<sup>28</sup> However, the calculated  $\beta_x$ -values provide a reversed result.

$\beta$  of a  $m$ -NA molecule may be decomposed into two parts<sup>10,32</sup>

$$\beta = \beta_{\text{add}} + \beta_{\text{ct}} \quad (16)$$

where  $\beta_{\text{add}}$  is due to the benzene ring-radical interactions and is thus additive with respect to the contribution of each substituent and  $\beta_{\text{ct}}$  is due to the donor-acceptor CT of  $\pi$ -electrons. The frontier orbital analysis described above suggests, in III, that the shift toward smaller  $\pi$ -electron-donating character of the HOMO does not contribute to enhancement of the  $\beta_x$ -value. However, such polarized  $\pi$ -electrons repel  $\sigma$ -electrons, causing a reversed polarization of these electrons.<sup>27,33</sup> It has been analyzed that this reversed polarization is derived from an interaction of the  $\pi$ -electrons of the aromatic

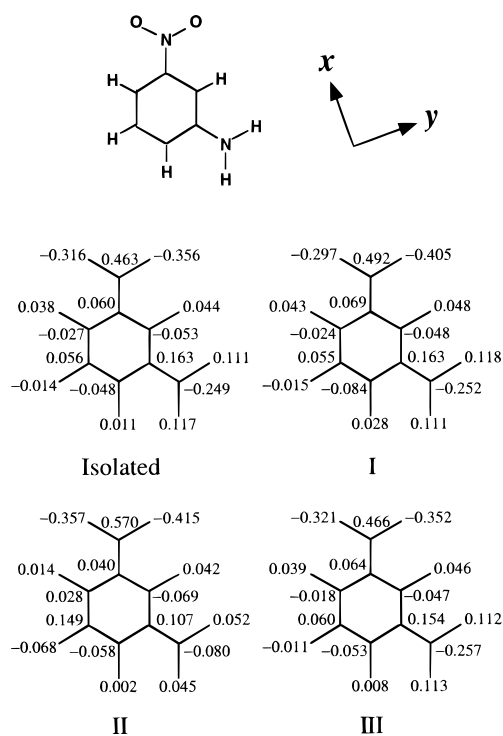


**Figure 5.** Net atomic charges of an isolated molecule and of a reference molecule in the model  $m$ -NA crystals studied in the absence of a static electric field.

hydrocarbon with a  $p\pi$ -nonbonding orbital.<sup>33</sup> Such an interaction occurs for the HOMO in III, since the  $p\pi$ -nonbonding orbital  $\phi^{(N)}$  contributes to the HOMO as shown in Table 3. This reversed polarization might more than compensate for the shift of the HOMO since reversed polarization here means enlargement of the donor character due to the inductive effect of  $\sigma$ -electrons in the ground state. The increase in  $\beta$  would then arise from the  $\beta_{\text{add}}$ -term.

However, the differences in the  $\beta_x$ -values could not be sufficiently explained only by the reversed polarization of the  $\sigma$ -electrons. This is because the effect of  $\sigma$ -electrons on  $\beta$  is an order of magnitude smaller than that of  $\pi$ -electrons; the ratio of the  $\beta$  due to  $\sigma$ -electrons to that due to  $\pi$ -electrons was reported to be *ca.* one-third in a  $m$ -NA molecule.<sup>34</sup> In the next subsection, after confirmation of the effect of the reversed polarization, a further analysis is presented in order to clarify the effect of the different crystal environments on the  $\beta_x$ -values.

**3.2.3.  $\mu_x$  and Net Atomic Charges.** To manifest the relation between the reversed polarization and the  $\beta_x$ -value, net atomic charges were analyzed. Figure 5 displays net atomic charges of an isolated molecule and of a reference molecule in the model  $m$ -NA crystals studied in the absence of a static electric field. The net atomic charge on the nitrogen atom of the  $\text{NH}_2$  group of II is much smaller than the others, while the net charge on the  $\text{NO}_2$  group does not show an equivalent effect. This smaller charge on the nitrogen atom of II is derived from the larger repulsive interaction of the  $\text{NH}_2$  group with the  $\text{NH}_2$  group of the adjacent molecule located below as shown in Figure 2. By this repulsive interaction the HOMO and LUMO levels of II get more destabilized than the others, as shown in Table 4. Note that the nitrogen atom of the  $\text{NH}_2$  group of III is subject not only to the repulsive interaction but also to the attractive interaction by the  $\text{NO}_2$  group of the next adjacent molecule, leading to the larger charge on the nitrogen atom of III than is the case in II. On the other hand, the  $\text{NO}_2$  group is predominantly subject to the attractive interaction by the  $\text{NH}_2$  group of the neighboring molecule in all the model crystals studied.

**TABLE 5:  $\mu_x$ -Values (D) of an Isolated Molecule and of the Reference Molecules in the Model *m*-NA Crystals Studied**

model <sup>a</sup>	$\mu_x(0)^b$	$\mu_x(E_x)^c$	$\mu_x(-E_x)^d$	$\mu_x(E_x) - \mu_x(0)$	$\mu_x(-E_x) - \mu_x(0)$
isolated	6.747	6.230	6.262	-0.517	0.515
I	8.367	7.714	9.016	-0.653	0.649
II	8.582	7.921	9.242	-0.661	0.660
III	6.869	6.315	7.425	-0.556	0.554

<sup>a</sup> The model structures are shown in Figure 2. <sup>b</sup>  $\mu_x$ -Values in the absence of a static electric field. <sup>c</sup>  $\mu_x$ -Values with a static electric field of +0.001 au along the *x*-direction. <sup>d</sup>  $\mu_x$ -Values with a static electric field of -0.001 au along the *x*-direction.

In comparison with the net charges in II, net atomic charges of the oxygen atoms upon a NO<sub>2</sub> group and of the nitrogen atom upon an NH<sub>2</sub> group in III become more positive and more negative, respectively. This tendency of the electron localization (density) is just opposite to that of the  $\pi$ -electron localization on the HOMO, as pointed out in the previous section. It has been confirmed, therefore, that the reversed polarization of  $\sigma$ -electrons will come about by the polarized  $\pi$ -electrons since the  $\sigma$ -electrons contribute to the electron density. The same conclusion is also derived from a comparison with net atomic charges in I.

Thus, it has been pointed out that the strong local crystal field in III largely will influence the  $\beta_x$ -value additively ( $\beta_{\text{add}}$ ) accompanied by the change in charge density dominantly on the NO<sub>2</sub> and the NH<sub>2</sub> groups. This is supported by the fact that, in a *m*-NA molecule, the relative contribution of  $\beta_{\text{ct}}$  to  $\beta$  was estimated to be 5% by Zyss.<sup>34</sup> The change will be derived from the reversed polarization of the  $\sigma$ -electrons due to the polarized  $\pi$ -electrons.

In any donor-acceptor  $\pi$ -conjugated systems, there is a net polarization of the electronic ground state. This polarization can vary depending on the strength of the donor and acceptor groups and on the environments. This has been discussed in detail by the number of papers of Marder *et al.*<sup>35</sup> and the recent paper by Albert.<sup>36</sup> They have showed that the ground state polarization is indexed by the bond-length alternation (BLA), which is defined as the difference between the average single- and double-bond distances in the conjugated pathway. Thus the polarization could vary the BLA from a neutral polyene-like ground state electronic structure (polyene limit), through a partially ionic cyanine-like state (cyanine limit), to a fully charge-separated charge transfer state (zwitterionic limit) in the context of merocyanine.<sup>35</sup> In other words, the linear and nonlinear optical response properties could be well-understood by the degree of the ground state polarization, that is, by the extent of the charge separation. Therefore, the effect of the local crystal environments on the  $\beta_x$  was analyzed from this respect.

The degree of the ground state polarization was estimated by means of  $\mu_x$  with respect to a  $\beta_{\text{xxx}}$ -value, which is the main contributor to the  $\beta_x$ -value. Table 5 stands for  $\mu_x$ -values of the isolated molecule and of the reference molecules in the model *m*-NA crystals studied. Here  $\mu_x(0)$  is a  $\mu_x$ -value in the absence of a static electric field, and  $\mu_x(E_x)$  and  $\mu_x(-E_x)$  are  $\mu_x$ -values with a static electric field of  $\pm 0.001$  au along the *x*-direction. Quite interesting is that the  $\mu_x(0)$ -value in II is the largest of those for the model crystals studied whereas the sum of the  $\mu_x(E_x) - \mu_x(0)$  and the  $\mu_x(-E_x) - \mu_x(0)$  values is the smallest, which leads to the smallest  $\beta_{\text{xxx}}$ -value. The largest  $\mu_x(0)$ -value here means that the ground state is the most polarized, that is, a zwitterionic-like electronic state. This is confirmed by the fact that the total net charges on all the atoms of the NH<sub>2</sub> group and of the NO<sub>2</sub> group show positive (+0.017) and negative (-0.202) values, respectively, only for II. In this case, the

change in dipole moment between the ground and excited states will be small and hence a small  $\beta$ -value will be obtained,<sup>35a,35f</sup> which is consistent with the above result.

$\beta$  in a negative sense increases from the cyanine limit, peaks for an intermediate cyanine/zwitterionic state, and then decreases to become smaller in the zwitterionic limit.<sup>35</sup> The degree of the ground state polarization, estimated from the  $\mu_x(0)$ -value, decreases in the order of II > I > III > the isolated molecule. Thus, the ground state electronic structure goes from the cyanine limit of the isolated molecule to the zwitterionic limit of II in that order since all the  $\beta_{\text{xxx}}$ -values are negative. Thus, the  $\beta_{\text{xxx}}$ -value of I and of III should be larger than that of the isolated molecule and of II. The  $\beta_{\text{xxx}}$ -values obtained show the same result qualitatively. This result indicates that the variation of  $\beta_{\text{xxx}}$ -values depending on the different crystal fields closely mirrors the variations of the difference in the dipole moments of the ground and excited states.<sup>36</sup>

Therefore, it has been considered that the effect of the different crystal environments on the  $\beta_{\text{xxx}}$ -values will be well-explained by the degree of the ground state polarization. Namely, the ground state electronic structure of I and of III, which lies between the cyanine limit and the zwitterionic structures, gives the larger  $\beta_{\text{xxx}}$ -value than that of the isolated molecule (cyanine limit) and of II (zwitterionic limit).

#### 4. Conclusions

The VBWP method has been developed to study a permanent crystal field effect on  $\beta$  for van der Waals organic crystals. The method not only gives a total  $\mu$ -value with an accuracy comparable to the SM method but also has the advantage of calculating a  $\mu$ -value of each fragment molecule. The method has been applied to a *m*-NA molecule in its different crystal environments, by using the model crystals, to analyze well the crystal field effect on the  $\beta$ -values.

The results show that the  $\beta$ -values are very sensitive to an anisotropic influence of the local crystalline environment studied. The crystal field in III induces the intramolecular CT of the  $\pi$ -electrons from the NH<sub>2</sub> group to the NO<sub>2</sub> group in the HOMO, while the LUMO almost remains unchanged. From a net atomic charge analysis, the CT will be derived from the reversed polarization of the  $\sigma$ -electrons due to the polarized  $\pi$ -electrons and it will then contribute to the enhancement of the  $\beta_x$ -value additively ( $\beta_{\text{add}}$ ).

To clarify further the effect of the different crystal environments on the  $\beta_{\text{xxx}}$ -values, the ground state polarization was investigated in terms of the  $\mu_x$  and net atomic charges. The ground state electronic structure goes from the cyanine limit of the isolated molecule through the intermediate cyanine/zwitterionic state of I and of III to the zwitterionic limit of II. The intermediate state of I and of III shows that the larger  $\beta_{\text{xxx}}$ -value is larger than that of the cyanine limit of the isolated molecule and of zwitterionic limit of II. This result reflects the relation between a ground state polarization and  $\beta$  proposed by Marder *et al.*<sup>35</sup> It has been concluded, therefore, that the effect of the different crystal environments on the  $\beta_{\text{xxx}}$ -values will be well-elucidated by the degree of the ground state polarization.

In the crystalline *m*-NA molecule, the crystal field plays a significant role in determining the  $\beta$ -values. In polar crystals with H-bonding such as *m*-NA,  $\beta$  should be estimated to take permanent crystal fields into account.

**Acknowledgment.** The authors are grateful to Professor H. Fujimoto of Kyoto University for useful comments and discussions.

## References and Notes

- (1) (a) Kobayashi, T., Ed. *Nonlinear Optics of Organics and Semiconductors*; Springer-Verlag: Berlin, 1988. (b) Messier, J., Kajzar, F., Prasad, P., Eds. *Organic Molecules for Nonlinear Optics and Photonics*; NATO ASI Series; Kluwer Academic Publishers: London, 1990.
- (2) (a) Williams, D. J., Ed. *Nonlinear Optical Properties of Organic and Polymeric Materials*; ACS Symposium Series 233; American Chemical Society: Washington, DC, 1983. (b) Chemla, D. S., Zyss, J., Eds. *Nonlinear Optical Properties of Organic Molecules and Crystals*; Academic Press: New York, 1987; Vols. 1 and 2. (c) Prasad, P. N., Ulrich, D. R., Eds. *Nonlinear Optical and Electroactive Polymers*; Plenum Press: New York, 1988.
- (3) (a) Oudar, J. L.; Zyss, J. *Phys. Rev.* **1982**, A26, 2016. (b) Zyss, J.; Oudar, J. *Phys. Rev.* **1982**, A26, 2028.
- (4) Dirk, C. W.; Twieg, R. J.; Wagnière, G. *J. Am. Chem. Soc.* **1986**, 108, 5387.
- (5) Theiste, D.; Callis, P. R.; Woody, R. W. *J. Am. Chem. Soc.* **1991**, 113, 3260.
- (6) Zyss, J.; Berthier, G. *J. Chem. Phys.* **1982**, 77, 3635.
- (7) Dykstra, C. E.; Liu, S.-Y.; Malik, D. J. *J. Mol. Struct. (THEOCHEM)* **1986**, 135, 357.
- (8) (a) Hurst, M.; Munn, R. W. *J. Mol. Electron.* **1987**, 3, 75. (b) Hurst, M.; Munn, R. W. *J. Mol. Electron.* **1988**, 4, 31.
- (9) Wagnière, G. H.; Hutter, J. B. *J. Opt. Soc. Am. B* **1989**, 6, 693.
- (10) Oudar, J. L.; Chemls, D. S. *J. Chem. Phys.* **1977**, 66, 2664.
- (11) (a) Kurtz, S. K.; Perry, T. T. *J. Appl. Phys.* **1968**, 39, 3798. (b) Jerphagnon, J. *IEEE J. Quantum Electron.* **1971**, 7, 42. (c) Bergman, J. G.; Crane, G. R. *J. Chem. Phys.* **1977**, 66, 3803. (d) Carencio, A.; Jerphagnon, J.; Perigaud, A. *J. Chem. Phys.* **1977**, 66, 3806.
- (12) Skapski, A. C.; Stevenson, J. L. *J. Chem. Soc., Perkin Trans.* **1973**, 2, 1197.
- (13) Vinson, L. K.; Dannenberg, J. J. *J. Am. Chem. Soc.* **1989**, 111, 2777.
- (14) See, for example: Margenau, H.; Kestner, N. R. *Theory of Intermolecular Forces*; Pergamon Press: New York, 1971; p 148.
- (15) (a) Löwdin, P. O.; Pauncz, R.; de Heer, J. *J. Math. Phys.* **1960**, 1, 461. (b) Löwdin, P. O. *J. Math. Phys.* **1962**, 3, 963.
- (16) McWeeny, R. *Quantum Mechanics*; Pergamon press: Oxford, 1973; p 18.
- (17) Ziman, J. M. *Elements of Advanced Quantum Theory*; Cambridge University: Cambridge, 1969; p 53.
- (18) Löwdin, P. O. *J. Mol. Spectrosc.* **1964**, 14, 119.
- (19) Bulk, G.; Jelitto, R. *J. Phys. Lett.* **1988**, 133, 231.
- (20) Kurtz, H. A.; Stewart, J. J. P.; Dieter, K. M. *J. Comput. Chem.* **1990**, 11, 82.
- (21) Pople, J. A.; Segal, G. A. *J. Chem. Phys.* **1966**, 44, 3289.
- (22) Sadlej, J. *Semiempirical Methods of Quantum Chemistry*; Ellis Harwood Limited: Chichester, England, 1985; pp 93–94, 142–160.
- (23) Segal, G. A., Ed. *Semiempirical Methods of Electronic Structure Calculation, Part A*; Plenum Press: New York, 1977; p 40.
- (24) Caron, A.; Donohue, J. *Acta Crystallogr.* **1964**, 17, 544.
- (25) Murrell, J. N.; Randic, M.; Williams, D. R. *Proc. R. Soc.* **1965**, A284, 1293.
- (26) (a) Papadopoulos, M. G.; Waite, J.; Nicolaidis, C. A. *J. Chem. Phys.* **1982**, 77, 2527. (b) Waite, J.; Papadopoulos, M. G. *J. Chem. Phys.* **1985**, 82, 1427.
- (27) Velders, G. J. M.; Gillet, J.-M.; Becker, P. J.; Feil, D. *J. Phys. Chem.* **1991**, 95, 8601.
- (28) Tsunekawa, T.; Yamaguchi, K. *J. Phys. Chem.* **1992**, 96, 10268.
- (29) Keshari, V.; Karna, S. P.; Prasad, P. N. *J. Phys. Chem.* **1993**, 97, 3525.
- (30) Nobutoki, H.; Koezuka, H. *J. Phys. Chem.* **1996**, 100, 6451.
- (31) (a) Fujimoto, H.; Hoffmann, R. *J. Phys. Chem.* **1974**, 78, 1874. (b) Imamura, A.; Hirano, T. *J. Am. Chem. Soc.* **1975**, 97, 4192.
- (32) Levine, B. F. *Chem. Phys. Lett.* **1976**, 37, 516.
- (33) (a) Murrell, J. N. *The Theory of the Electronic Spectra of Molecules*; Wiley: New York, 1963. (b) Zyss, J. *J. Chem. Phys.* **1979**, 70, 3341.
- (34) Zyss, J. *J. Chem. Phys.* **1979**, 71, 909.
- (35) (a) Marder, S. R.; Beratan, D. N.; Cheng, L.-T. *Science* **1991**, 252, 103. (b) Marder, S. R.; Cheng, L.-T.; Tiemann, B. G.; Friedli, A. C.; Blanchard-Desce, M.; Perry, J. W.; Skindhoj, J. *Science* **1994**, 263, 511. (c) Marder, S. R.; Perry, J. W.; Bourhill, G.; Gorman, C. B.; Tiemann, B. G. *Science* **1993**, 261, 183. (d) Marder, S. R.; Gorman, C. B.; Perry, J. W.; Bourhill, G.; Brédas, J.-L. *Science* **1994**, 265, 632. (e) Marder, S. R.; Gorman, C. B.; Tiemann, B. G.; Cheng, L.-T. *J. Am. Chem. Soc.* **1993**, 115, 3006. (f) Meyers, F.; Marder, S. R.; Pierce, B. M.; Brédas, J. L. *J. Am. Chem. Soc.* **1994**, 116, 10703. (g) Gorman, C. B.; Marder, S. R. *Proc. Natl. Acad. Sci. U.S.A.* **1993**, 90, 11297.
- (36) Albert, I. D. L.; Marks, T. J.; Ratner, M. A. *J. Phys. Chem.* **1996**, 100, 9714.